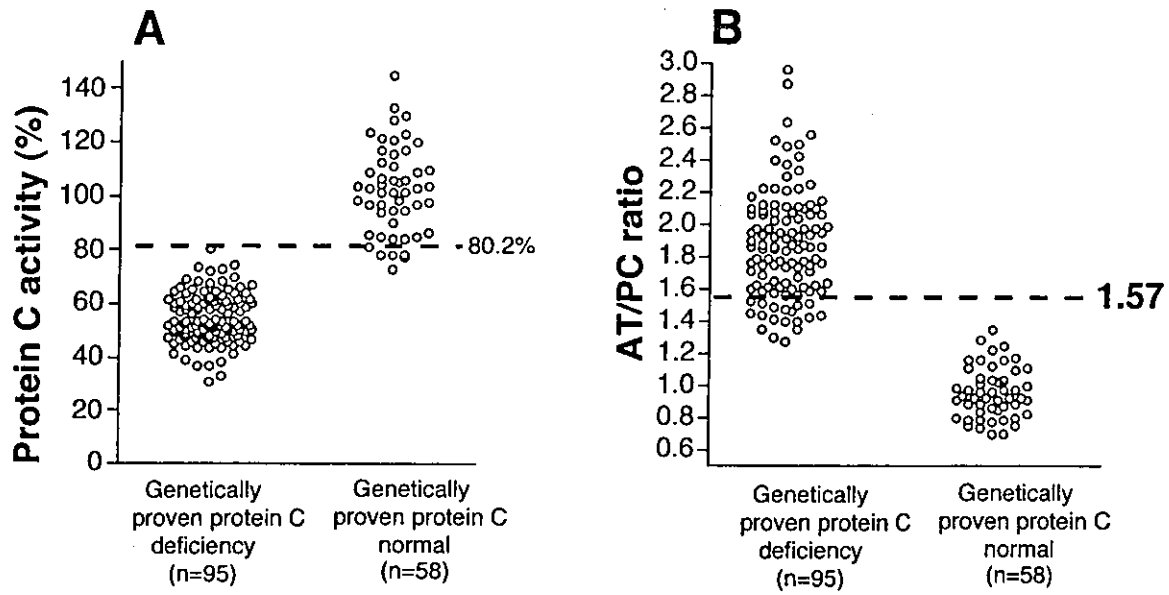

Fig. 3 Distribution of protein C activity (A) and antithrombin/protein C ratio (B) in genetically proven protein C deficiency and in genetically proven protein C normal.

Table Comparison of prevalence of protein C and antithrombin deficiencies between deep vein thrombosis group and general population

	Number of protein C heterozygote	Number of antithrombin heterozygote
General population (n = 4505)	9 (0.20 %)	8 (0.18 %)
Patients with DVT (n = 108)	7 (6.5 %)	6 (5.6 %)
Odds ratio (95 % CI)	34.6 (12.64 to 94.82)	31.3 (11.27 to 97.06)
P value	< 0.0001	< 0.0001

CI; confidence interval

め，これまで遺伝子解析[7]でPCの遺伝子変異部位が同定された患者およびその家系員と遺伝子変異部位が同定されなかったPC正常者間で同様の検討を行った(**Fig. 3**)．その結果，PC正常者でAT/PC活性比>1.57を示す者はおらず，PC欠乏症では大部分がAT/PC活性比>1.57を示した．このことから今回の研究で用いたPC欠乏症のcriteria(AT/PC活性比>1.57)が妥当であることが示唆された．しかし，PC欠乏症であってもAT/PC活性比が1.57以下の症例もあり，AT/PC活性比のcut-off値を>1.57とした場合，これらの症例はPC正常者に分類され，PC欠乏症の頻度が低く算出される可能性があることを認識しておく必要がある．この結果からOdds ratioは約35となり，PC欠乏症がDVT発症の極めて大きなリスクファクターとなることが示された(**Table**)．

今回我々が求めた一般住民におけるPC欠乏症の頻度は，欧米での頻度(0.15～0.33%)と一致することが分かった[8]．一方，本研究における日本人の静脈血栓症患者でのPC欠乏症の頻度(6.5%)は，欧米人の3.2%に比べ高頻度であった．これは，欧米人ではプロトロンビンG20210Aや第V因子Leidenなどの遺伝子多型が静脈血栓症発症の主な要因となり，PCやAT欠乏症による静脈血栓症発症者の割合が低くなったと考えられる．日本人においてはplasminogen異常症が多く認められるものの血栓症発症の強いリスクファクターとはならず，プロトロンビンG20210Aや第V因子Leidenなどの遺伝子多型が存在しないことからPCやAT欠乏症による静脈血栓症発症者の割合が高くなったと考えられる．

2．AT欠乏症

PCと同様の対象(n =4505)でAT欠乏症の頻度を求め

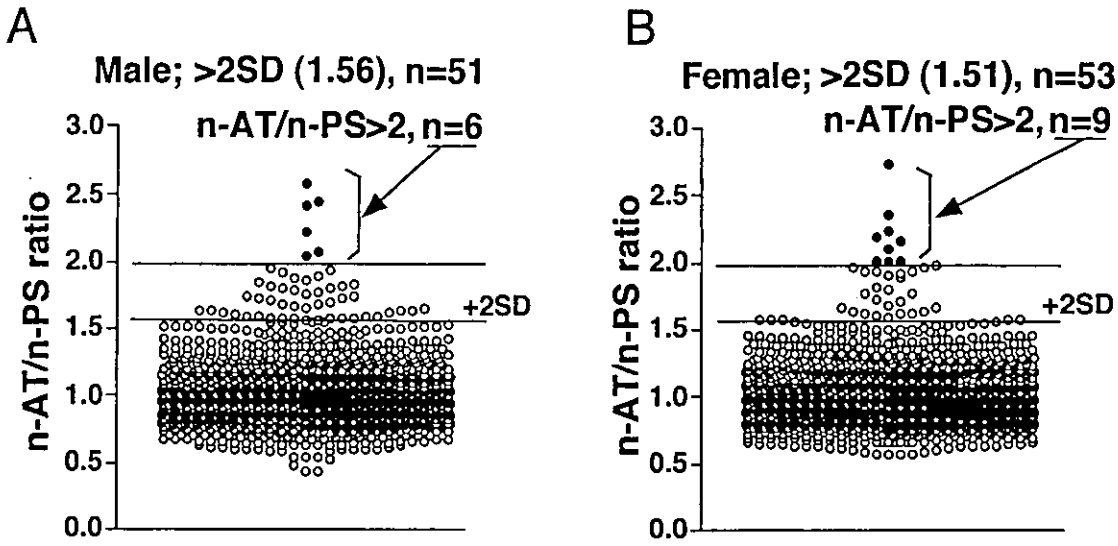

Fig. 4　Distribution of normalized antithrombin/normalized protein S activity (n-AT/n-PS) ratio by sex.
A; Male, B; Female.

た．AT欠乏症のcriteriaはPC / AT活性比≧1.67およびAT活性<75%を満たす者とした．その結果，一般住民およびDVT患者における頻度はそれぞれ 8 名(8 / 4505，0.18%)，6名(6/108，5.6%)となった(Table)．

一般住民におけるAT欠乏症の頻度は，本研究における日本人(0.18%)と欧米人(0.17%)との間で極めてよく一致した[8]．しかし，静脈血栓症患者での頻度はPC欠乏症と同様，欧米人のもの(1.1%)より本研究における日本人において高頻度であった．この原因もPC欠乏症で述べた要因によるものと考えられる．最近の米国で行われた前向き研究では，AT欠乏症は静脈血栓症の危険因子ではないとされており[4]，日本においてもこのような前向き研究が必要と思われる．

3．PS欠乏症

PS欠乏症は4505名の内，2690名のPS活性を凝固法により測定した．男女別々にAT活性とPS活性の平均値が100%となるように標準化した後，標準化－AT/標準化－PS(以下，n-AT / n-PS活性比)の分布をFig. 4に示した．n-AT/n-PS活性比が2SD以上(男性1.56，女性1.51)を示した者は男性51名，女性53名であった．また，n-AT / n-PS活性比が 2 以上を示した者は，男性 6 名，女性 9 名であった．PS欠乏症のcriteriaをn-PS<mean-2SDおよびn-AT / n-PS活性比> 2SDを満たす者とした場合，PS欠乏症の頻度は1.44%となった．また，n-AT / n-PS活性比> 2 以上とした場合，0.56%となった．

今回の研究で得られたPS欠乏症の頻度は，これまでの日本人健常人(n = 392)を対象とした研究結果(2.8%)とほぼ一致し[9]，日本人におけるPS欠乏症の頻度はPCやAT欠乏症より高頻度となることが明らかとなった．しかし，日本人一般住民におけるPS欠乏症の頻度(0.56%～1.44%)はスコットランドで求められた頻度0.03～0.13%より高かった[10]．これは日本人に多く見られるLys155Glu変異(PS 徳島)によるものと考えられる[11]．

4．APCレジスタンス

日本人における第 V 因子Leiden変異の報告はまだない．しかし，われわれは第 V 因子Leiden非依存性のAPCレジスタンス，即ち，後天性のAPCレジスタンスが動静脈血栓症において認められることを報告した[12]．Fig. 5は健常人(n=180)および各疾患患者(DVT；n=28，肺塞栓症；n = 15，脳梗塞；n = 41，冠動脈疾患；n = 14)におけるAPCレジスタンスの値をプロットしたもので，APCレジスタンスは標準化APC感受性比(normalized-APC-sensitivity ratio，n-APC-SR)として示した．第 V 因子Leidenを有する場合，n-APC-SRが0.7以下を示すことが知られており[13]，今回の研究で動静脈血栓症患者群においてn-APC-SR<0.7を示す者が数名見られた．

また，Fig. 6にAPCレジスタンスと活性型凝固第VII

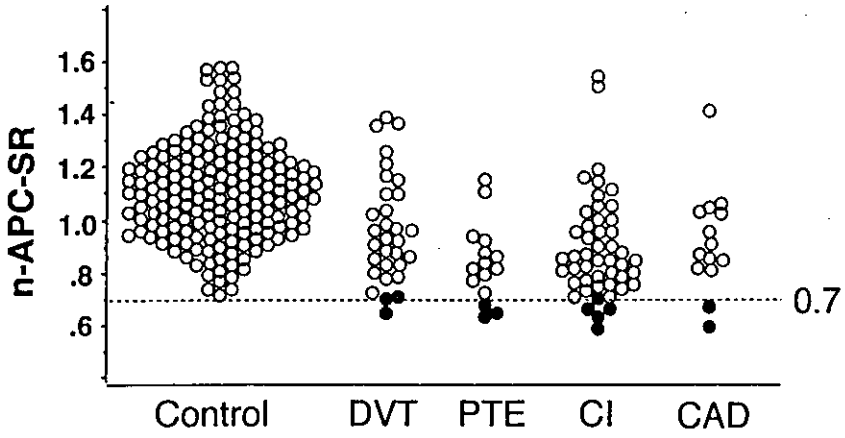

Fig. 5 Distribution of normalized APC resistance.
n-APC-SR: normalized activated protein C sensitivity ratio, DVT: deep vein thrombosis, PTE: pulmonary thromboembolism, CI: cerebral infarction, CAD: coronary artery disease.

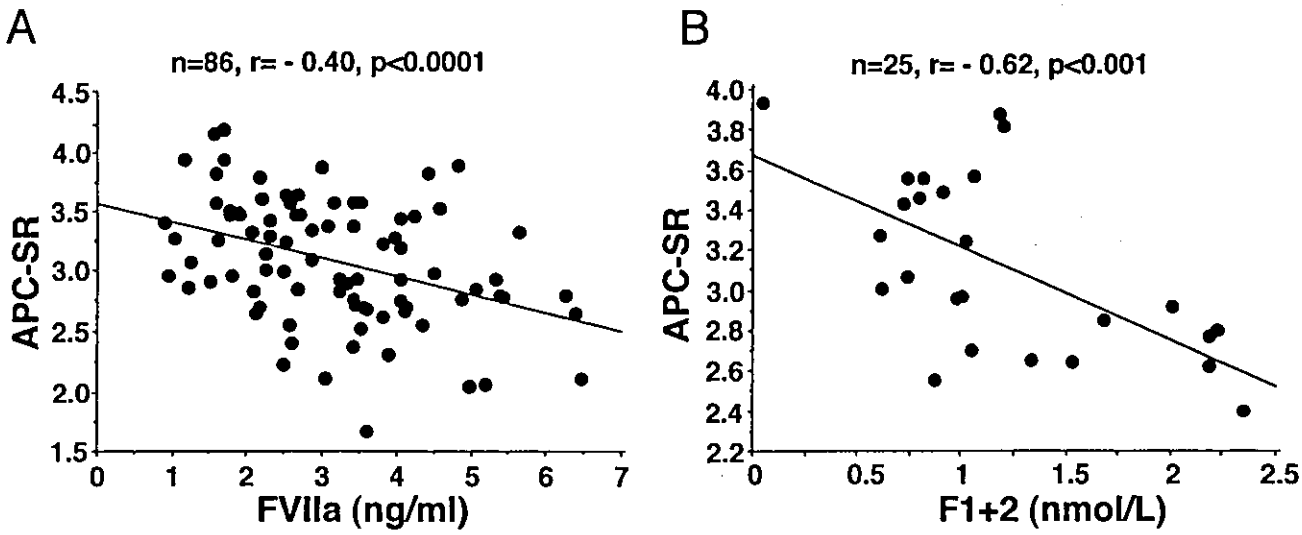

Fig. 6 Relationship between APC resistance and activated factor VII (A) or prothrombin fragment 1+2 (B).
APC-SR: activated protein C-sensitivity ratio, FVIIa: activated factor VII, F1+2: prothrombin fragment 1+2.

因子(FVIIa)およびProthrombin fragment1＋2(F1＋2)との関係を示した．血漿中FVIIaは組織因子との複合体を形成することにより外因系凝固反応を惹起することが知られており，動脈硬化性疾患で血漿中FVIIa濃度が高値となる[14]．また，F1＋2はプロトロンビンが活性型第X因子により活性化を受ける際に生成される．動静脈血栓症患者においてAPC-SRはFVIIa(n = 86，r = -0.40，P<0.0001)やF1＋2(n = 25，r = -0.62，P<0.001)と有意な負の相関が認められた．これらの結果は，APCレジスタンスの存在が過凝固状態であることを示していると考えられる．従って，日本人においては第V因子Leiden変異がなくても後天性APCレジスタンスが静脈血栓症のリスクファクターとなる可能性があると考えられる．

おわりに

日本人における先天性血栓性素因としてPCやATT欠乏症が重要と考えられる．また，PS欠乏症は日本人に多く見られるが，静脈血栓症のリスクファクターとしての重要性について，今後の研究が期待される．第V因子Leiden非依存性APCレジスタンスも静脈血栓症のリスクファクターとなる可能性があり，血栓検査のscreening項目として必要と考えられる．

文 献

1) Rosendaal, F. R., Doggen, C. J. M., Zivelin, A., et al.: Geographic distribution of the 20210 G to A prothrombin variant. Thromb. Haemost., 1998, **79**: 706-708.
2) Nicolaes, G. A. F. and Dahlbäck, B.: Factor V and thrombotic disease. Description of a Janus-faced protein. Arterioscler. Thromb. Vasc. Biol., 2002, **22**: 530-538.
3) Sanson, B.-J., Simioni, P., Tormene, D., et al.: The incidence of venous thromboembolism in asymptomatic carriers of a deficiency of antithrombin, protein C, or protein S: a prospective cohort study. Blood, 1999, **94**: 3702-3706.
4) Folsom, A. R., Aleksic, N., Wang, L., et al.: Protein C, antithrombin, and venous thromboembolism incidence: a prospective population-based study. Arterioscler. Thromb. Vasc. Biol., 2002, **22**: 1018-1022.
5) Miyata, T., Kawasaki, T., Fujimura, H., et al.: The prothrombin gene G20210A mutation is not found among Japanese patients with deep vein thrombosis and healthy individuals. Blood Coagul. Fibrinolysis, 1998, **9**: 451-452.
6) Fujimura, H., Kambayashi, J., Monden, M., et al.: Coagulation factor V Leiden mutation may have a racial background. Thromb. Haemost., 1995, **74**: 1381-1382.
7) Sakata, T., Kario, K., Katayama, Y., et al.: Studies on congenital protein C deficiency in Japanese: prevalence, genetic analysis, and relevance to the onset of arterial occlusive diseases. Semin. Thromb. Hemost., 2000, **26**: 11-16.
8) De Stefano, V., Finazzi, G. and Mannucci, P. M.: Inherited thrombophilia: pathogenesis, clinical syndromes, and management. Blood, 1996, **87**: 3531-3544.
9) Nomura, T., Suehisa, E., Kawasaki, T., et al.: Frequency of protein S deficiency in general Japanese population. Thromb. Res., 2000, **100**: 367-371.
10) Dykes, A. C., Walker, I. D., McMahon, A. D., et al.: A study of protein S antigen levels in 3788 healthy volunteers: influence of age, sex and hormone use, and estimate for prevalence of deficiency state. Br. J. Haematol., 2001, **113**: 636-641.
11) Yamazaki, T., Sugiura, I., Matsushita, T., et al.: A phenotypically neutral dimorphism of protein S: the substitution of Lys155 by Glu in the second EGF domain predicted by an A to G base exchange in the gene. Thromb. Res., 1993, **70**: 395-403.
12) Sakata, T., Kario, K., Katayama, Y., et al.: Clinical significance of activated protein C resistance as a potential marker for hypercoagulable state. Thromb. Res., 1996, **82**: 235-244.
13) De Ronde, H. and Bertina, R. M.: Laboratory diagnosis of APC-resistance: a critical evaluation of the test and the development of diagnostic criteria. Thromb. Haemost., 1994, **72**: 880-886.
14) Kario, K., Matsuo, T., Kobayashi, H., et al.: Factor VII hyperactivity and endothelial cell damage are found in elderly hypertensives only when concomitant with microalbuminuria. Arterioscler. Thromb. Vasc. Biol., 1996, **16**: 455-461.

Abstract

Relationship between Functional Abnormality of Anticoagulant Factors and Venous Thrombosis in Japanese

Toshiyuki Sakata[1], Hiroshi Matsuo[2], Akira Okamoto[1] and Toshifumi Mannami[3]

1 Laboratory of Clinical Chemistry, National Cardiovascular Center, Osaka, Japan
2 Department of Cardiology, National Cardiovascular Center, Osaka, Japan
3 Department of Preventive Cardiology, National Cardiovascular Center, Osaka, Japan

Key words : Protein C deficiency, Antithrombin deficiency, Deep vein thrombosis, Risk factor

Protein C and antithrombin deficiencies are risk factors for venous thrombosis. The prevalence of protein C and antithrombin deficiencies is about 0.2% in the general population. These studies are mainly conducted in Caucasian population and not in Mongolian population such as Japanese. We examined the prevalence of these deficiencies in Japanese and whether or not these deficiencies are risk factors for deep vein thrombosis in Japanese. We measured the protein C and antithrombin activities in 4,505 individuals in the Japanese general population and in 108 patients with deep vein thrombosis, identified protein C and antithrombin, and compared their prevalences. The prevalence of protein C or antithrombin in general population was 0.20% or 0.18%, respectively. We identified 7 patients with protein C deficiency (6.5%) and 6 patients with antithrombin deficiency (5.6%) in 108 patients with deep vein thrombosis. These findings indicate that either protein C or antithrombin deficiency constitutes a significant risk factor for deep vein thrombosis in the Japanese population.

Jpn. J. Phlebol., 14 (5) : 339-345, 2003

Journal of Cerebral Blood Flow & Metabolism
23:821–828 © 2003 The International Society for Cerebral Blood Flow and Metabolism
Published by Lippincott Williams & Wilkins, Inc., Baltimore

Dynamic Observation of Oxygenation-Induced Contraction of and Transient Fiber-Network Formation–Disassembly in Cultured Human Brain Microvascular Endothelial Cells

*Kouji Inoue, *Minoru Tomita, *Yasuo Fukuuchi, *Norio Tanahashi, †Masahiro Kobari, *Masaki Takao, *Hidetaka Takeda, and ‡Masako Yokoyama

**Department of Neurology, School of Medicine, Keio University, †Department of Neurology, Tachikawa Hospital, and ‡Mitukoshi Sinryoujo, Tokyo, Japan*

Summary: Oxygenation-induced contraction of nonconfluent cultured human brain microvascular endothelial cells (HBECs, n = 30) was examined by video-enhanced contrast-differential interferential contrast microscopy. After administering a continuous gentle blow of pure oxygen gas to the surface of the medium just above the flattened HBEC, the plasma membrane exhibited tensioning and wrinkling, resulting in a strong contraction of the cell body by 14 ± 7% ($P < 0.001$). When the cell stopped contracting, transient formation of a fiber network starting from certain spots (possibly adhesion plaques, though these were not visible in the majority of cases) and expanding to the whole cell was observed. The occurrence of fiber network formation was statistically significant (26 of 30 separate cells, $P < 0.05$). After cessation of oxygen delivery, the observed network of fibers broke up rapidly (in a period of 3.3 ± 1.2 seconds) into small particles of <0.5 μm in diameter, which subsequently fused into the cellular structure. The HBEC completely recovered the control appearance. The sequential process was completed within 30 seconds and was reproduced in individual cells each time that oxygen gas was supplied. The authors conclude that the HBEC strongly contracts in response to a transient oxygenation stimulus, followed by rapid formation/disassembly of a network structure. **Key Words:** VEC-DIC microscopy—Human brain microvascular endothelial cell—Cytoskeleton—Cell morphology—Actin filament—Endothelial cell tone.

The mechanisms underlying hyperoxygenation-induced changes in tissue blood flow remain poorly understood despite a long history of investigation (Hudetz, 1997; Kety and Schmidt, 1948; Krogh, 1918; Meyer and Gotoh, 1961; Opitz and Schneider, 1950). Based on continuous recording of respiratory gases in arterial blood and jugular venous blood, Meyer et al. (1967) found that pure oxygen gas inhalation produced a marked arterial Po_2 rise by 365 mm Hg (from 70.8–435.0 mm Hg, n = 6), whereas the brain tissue Po_2 rose by only 9.0 mm Hg (from 25.8–34.7 mm Hg, n = 4) in men. It seemed highly likely that oxygen directly constricted pial arterioles but, strangely, no explicit evidence was forthcoming (Purves, 1972). This contrasted to the effect of hypoxia, which dilated the pial arteries in cats (Craigen Jennett, 1981). Recently, Sjoberg et al. (1999) reported that the cerebrocortical capillary blood flow was reduced by 11% during hyperoxemia, as measured by a hydrogen clearance method in anesthetized pigs. These data indicate that oxygen causes a selective reduction in blood flow at specific flow levels.

To examine the response of cultured human brain microvascular endothelial cells (HBECs) to high oxygen levels, we used video-enhanced contrast-differential interference contrast (VEC-DIC) microscopy, which enabled us to observe cultured cells in a living state at high magnification (Tomita et al., 1996*a*). With this technique, we have already shown that cultured human umbilical cord vein endothelial cells (HUVECs) contracted by approximately 20% on exposure to hyperoxygenated superfusing fluid (Tomita et al., 1995). In the present paper, we report the occurrence of a similar contraction in the HBEC in response to oxygen. However, in the present study we also observed a peculiar fiber network formation/disassembly process in the HBEC, in association with the contraction. Therefore, we describe for the

Received October 10, 2002; final revision received December 23, 2002; accepted February 3, 2003.

This study was supported by a research grant from the New Energy and Industrial Technology Development Organization, Tokyo, Japan.

Address correspondence and reprint requests to Dr. Minoru Tomita, Department of Neurology, School of Medicine, Keio University, 35 Shinanomachi, Shinjuku-ku, Tokyo 160–8582, Japan; e-mail: mtomita@sc.itc.keio.ac.jp

DOI: 10.1097/01.WCB.0000063992.19746.CA

first time dynamic morphologic changes of HBECs that are apparently of essential importance for the vasoactive behavior of capillaries, which until now have been considered to be rather passive and quiescent.

MATERIALS AND METHODS

Human brain microvascular endothelial cells of passage 2 were purchased from Dainippon Pharmaceutical Co., Ltd. (Osaka, Japan), which had imported cryopreserved cells (#376) from Cell Systems Corporation (Cambrex Corp., East Rutherford, NJ, U.S.A.). The cells were confirmed to be endothelial cells on the basis of low-density lipoprotein uptake and positive von Willebrand factor/factor VIII. Cells were seeded onto polystyrene dishes (Corning Petri dishes) containing a 175-μm thick glass coverslip coated with attachment factor (Cell Systems Corporation), and incubated in a humidified 5% CO_2/95% O_2 atmosphere at 37°C. The medium (Dulbecco modified Eagle medium: 45% + F12 45% + fetal bovine serum 10% + b-FGF 10 ng/mL) without astroglial cell supplement was changed every day, and observations were made at the fourth day after seeding. The coverslip with endothelial cells was attached with glue to a plastic dish, the bottom of which had a round window, so as to form the floor of a microscopic observation chamber (containing the cells). The dish was placed in a temperature-controlled metal housing unit to maintain the cell temperature at 37°C, and the coverslip was mounted on the objective lens of an inverted microscope with oil, so that subsequent video pictures would capture the ventral side of the cell. The cells were superfused continuously with the culture medium using a double pump system (infusion and suction pumps) and were maintained at 37°C in the microscopic observation chamber with a small heating pad and thermostat. Video images of the cells were contrast enhanced digitally in real time using our VEC-DIC microscopy technique at ×4000 using a halogen lamp with an ultraviolet-cut filter (Tomita et al., 1996a). A preparation of HBECs was set in place and a spread cell was selected for observation of morphologic changes. The amount of medium submerging the cell was adjusted so that the medium surface was apparently situated close to the vertex of the cell nucleus. Since the cell body was very flat (except for the nuclear region), approximately 5 (3–10) μm at the vertex and tapering to 0.3 μm at the peripheral part (Inoue et al. 1999), the surface of the medium was approximately 50 μm above the floor. After waiting for a certain period for control observation (20 minutes to 1 h), pure oxygen gas was blown gently onto the surface of the medium through an injection needle (#26), which was directed towards the cell at an angle of 30 degrees. The speed of gas introduction was a few milliliters per minute, which was so slow that ripples on the surface of the medium were barely visible. The period of oxygenation was usually less than 1 minute. This method was adopted because the previous method of superfusion with an oxygenated fluid involved a delay in the carrying tube and led to smearing of oxygen tension changes. Cell morphologic changes were videotaped, and selected parts of the images were further fed into a computer via a frame grabber card (Scion Corporation, Frederick, MD, U.S.A.) at frame rates of 2 to 15 frames/s (2–15 Hz) for analysis of details of the morphologic changes. The oxygen tension of the medium was monitored with a platinum electrode (applied potential: −0.5 V) with reference to an Ag-AgCl electrode. Although the medium was usually superfused slowly through the observation chamber with the infusion pump at the inlet and the suction pump at the outlet, observations were made mostly under static conditions of the fluid with a momentary (≤3 minutes) stoppage of the pumps. As described in Results, we confirmed that no changes in cell morphology occurred with changes in wall shear rate, which was altered by adjustment of the pump speed so as to be from 0 to 200 μm/s (the wall shear rate was calculated from the fluid thickness and volume flow passing through the chamber, assuming Newtonian properties of the superfusing fluid). To exclude other physical factors, the following were tested: fluid removal by using tissue paper; changes of temperature from 10°C to 40°C by controlling the thermostat of the circulating water; and vibration of the fluid by blowing air into the liquid. Electrical stimulation with a square pulse/triangular pulse (0.5 to 3.0 V DC/AC at frequencies of 1–100 Hz) was provided through a pair of bipolar electrodes placed in the medium above the cell.

For analysis of the rapid morphologic changes, subtraction between two frames was performed in some cases on a Scion domain by subtraction of the first image of the brain surface (control video image) from each subsequent experimental image (F-C subtraction), or by frame-by-frame subtraction in a series of frames (F-F subtraction). The contraction was broadly estimated from the diameter change of the cell body (%) as $(D_1^2-D_2^2)/D_1^2$, where D_1 is the control diameter measured at a line passing through the center of the cell and D_2 is that after the contraction. The magnification was about ×3,200 or 50 μm in the full width of the monitor window, and this was confirmed from the red blood cell size (7.5 μm). The speed of extension of network formation was estimated from the frame-by-frame differential distance (μm) divided by the frame interval (seconds).

RESULTS

The HBECs changed their shape depending on the phase of their growth. When HBECs at the fourth day after seeding, as used in the present study, were spread on a glass coverslip, they exhibited a broadly similar shape and size to those described previously for HUVECs (Inoue et al., 1999): a round-top nucleus containing one or two nucleoli, and a cell body surrounded by a thin, widely spread transparent marginal portion (Fig. 1, top left), forming various flat (lamellar) or projecting radial and spiky structures (lamellipodia and filopodia). The outer boundaries of the cell were usually not discernible with the naked eye but were visible as a mesh or bundles of fibers when the actin was stained with rhodamine phalloidin. HBECs were rather opaque and their intracellular organelles were not clearly visible, whereas the intracellular organelles of HUVECs could be observed; tubular structures (presumably mitochondria), vesicles, and large or small granules or particles that glided or were translocated in a vectorial fashion, presumably along the microtubules, were noted. However, we did not observe fiber formation in contracting HUVECs.

Typical morphologic changes in two independent cells in response to oxygenation are shown as montage presentations in Figs. 1 and 2. The numbers at the top left of

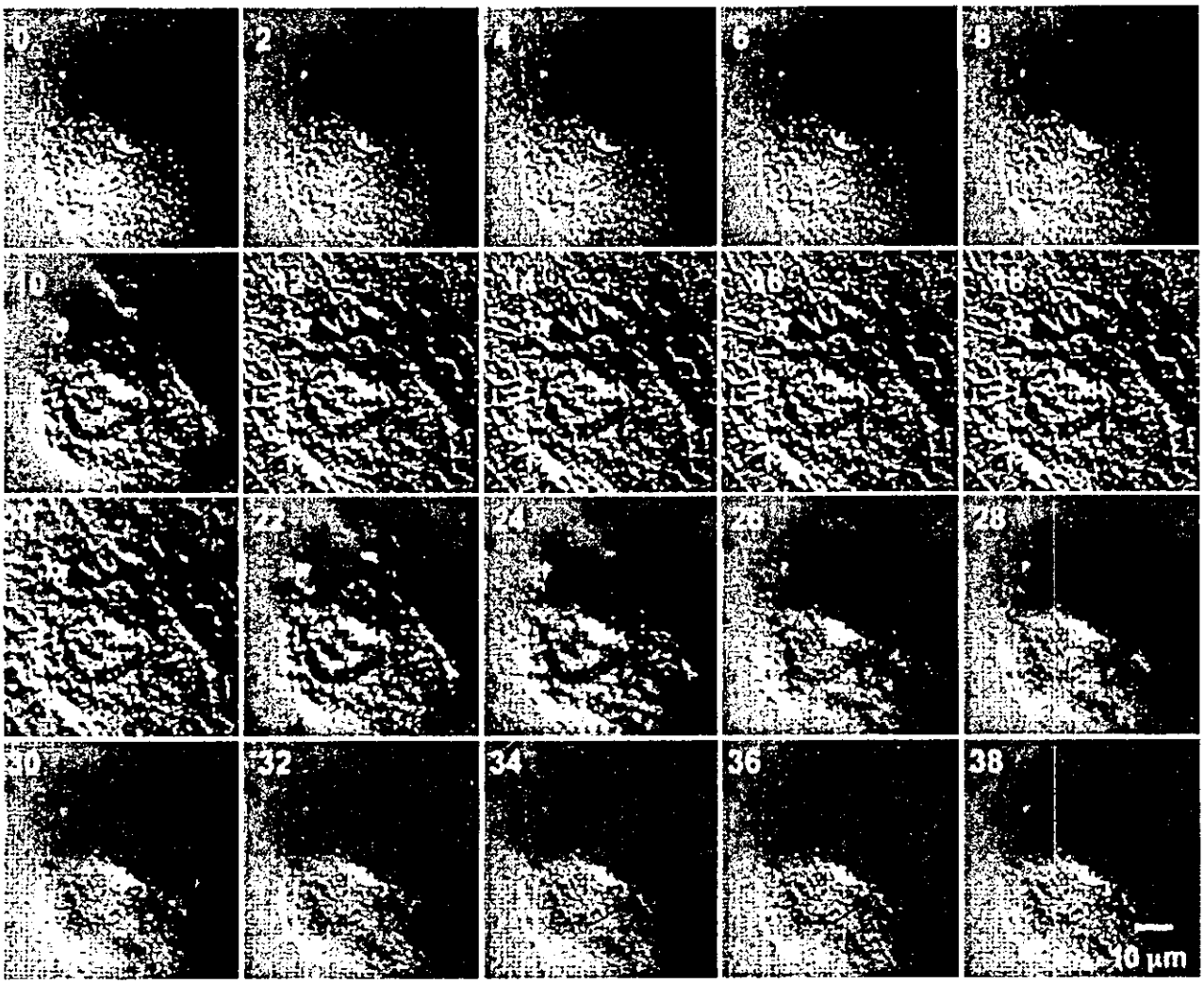

FIG. 1. Typical processes of contraction, wrinkling, mesh network formation, disassembly, and recovery as displayed in cell 9. The appearance time of the mesh network was 10 seconds, the duration was 12 seconds, recovery time was 20 seconds (10-second disassembly time + 10-second disappearance time), fiber thickness was 0.75 μm, spread speed was 10 μm/s, and contraction was 12% (shortening of the short axis of the cell from 25.0–23.6 μm). The mesh pattern was polygonal. Time (seconds) after oxygen delivery is indicated at the top-left of each frame. The endothelium exhibits a vaguely outlined nucleus (which becomes clearly apparent after contraction) containing a nucleolus in the center, a well-demarcated cell body, and the lamella, which occupies the outer skirt portion of the cell body.

each frame indicate the time in seconds after oxygen introduction. Within a few seconds after oxygen introduction, when the oxygen tension in the fluid reached a maximum (680 mm Hg), the cell began to contract. The surface tension of the plasma membrane appeared to increase, causing waves or wrinkles, especially in the circumferential area of the cell body. The peripheral lamella was dragged centrally towards the nucleus and the nuclear envelope became clearly demarcated and enhanced. The lamella became tightly wrapped around the edge of the cell body (frame 10 of Fig. 1 and frame 8 of Fig. 2). The cell body then began to contract and the maximum contraction was estimated from the reduction of the cell area as $14 \pm 7\%$ (mean $\pm$ SD, $P < 0.001$); nuclear size also decreased. When the contraction slowed down and stopped, a starlike mark suddenly appeared in nine cases as shown in Fig. 3. It started either at granules (top row of Fig. 3: presumably adhesion plaque) or at random spots without visible granules (middle and bottom rows of Fig. 3) and grew rapidly, like a spiderweb network. Figure 3 illustrates such expanding network structures as images obtained by F-F subtraction (middle row) and F-C subtraction (bottom row).

The fiber network started from spots that were presumably invisible adhesion plaques in the lamella binding to the coated glass surface. Figure 4 (top two rows, A–H) shows various types of mesh mosaic patterns of the network structures. These patterns were star shaped (A; n = 9), polygonal (B–E; n = 6), fernlike (F; n = 7), brushlike (G; n = 4), or evident of a augmented nuclear

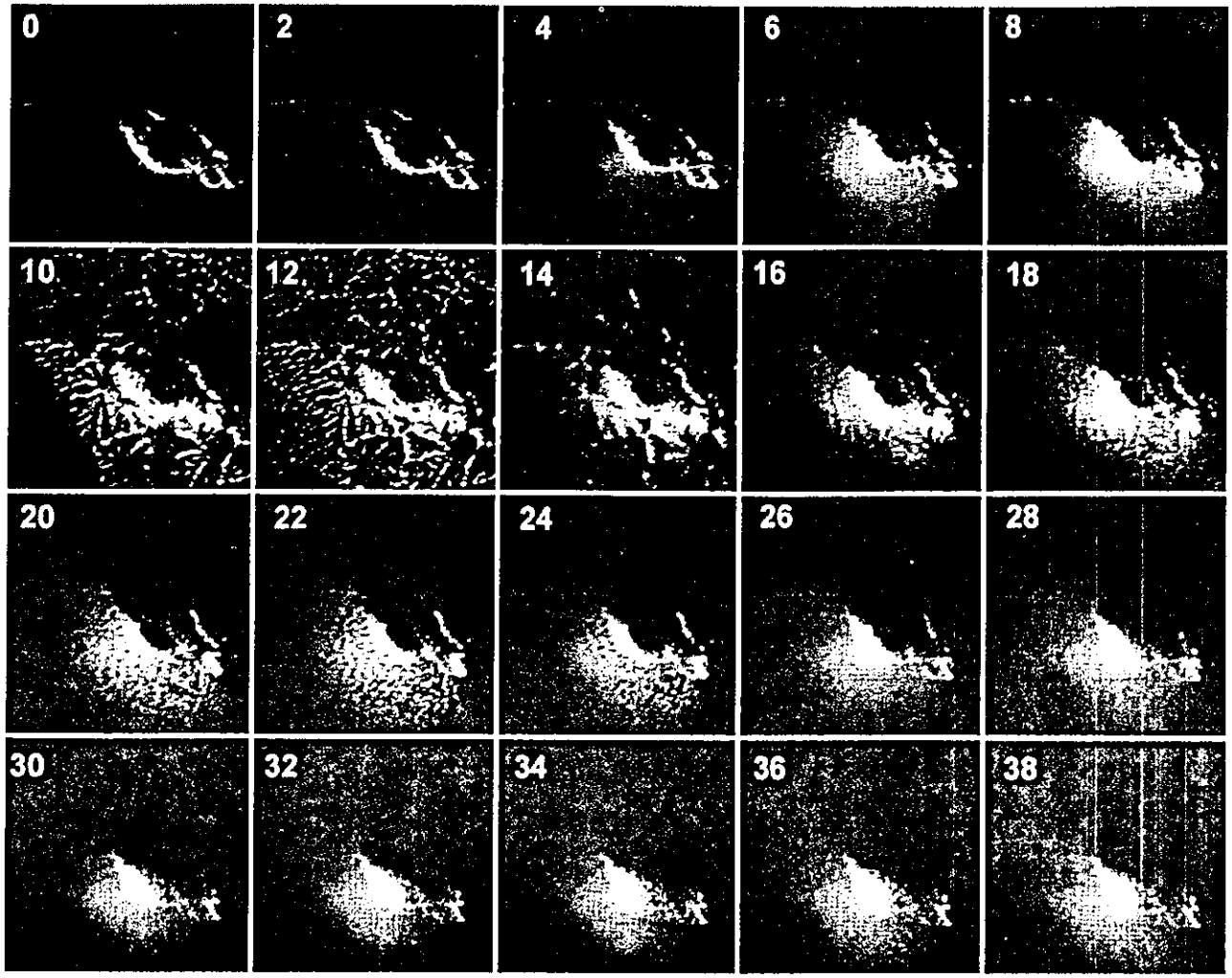

FIG. 2. Another typical process displayed in cell 11. The appearance time was 10 seconds, duration was 6 seconds, recovery time was 15 seconds (3-second disassembly time + 12-second disappearance time), fibers thickness was 0.75 μm, spread speed was 10 μm/s, and contraction was 14% (shortening of the long axis of the cell from 14.0–13.1 μm). The mesh pattern was starlike. The cell exhibits a rather deformed cell body with a deviated nucleus and tailed cell body.

envelope (H; n = 4); however, these classifications were not distinct and patterns overlapped in most cases. The average growth speed of the network was 16.3 ± 8.4 μm/s (mean ± SD). When the network was apparently fully formed, oxygen delivery was discontinued. As shown in Table 1, the average time from the commencement of oxygen exposure to the appearance of network formation was 6.5 ± 4.6 seconds, and the average duration of the network was 12.0 ± 7.8 seconds. The thickness of the mesh fibers in the network was 0.6 ± 0.2 μm. As soon as oxygen delivery was stopped (usually at full development of the network), the observed fibers rapidly began to disassemble into small particles (0.7 ± 0.2 μm in diameter) over a period of 3.3 ± 1.2 seconds, although this time is not reliable, since the oxygen tension changes in the fluid were smeared owing to saturation/evaporation processes. The small particles displayed a slow drift, exhibiting independent Brownian motion for a few seconds, and then disappeared, gradually becoming incorporated into the cell components (bottom row of Fig. 4). The cell shape recovered its original appearance, as shown in the last images of the two cells (Figs. 1 and 2). The overall recovery time, including disassembly time, was 12.6 ± 10.8 seconds. The process of HBEC morphologic change during oxygenation could (in 26 of 30 cases) be summarized as contraction-network formation in the cell to disassembly of fibers and particulation to recovery of the original cell shape, all occurring within 30 seconds. The sequential process was reproduced in all cases tested (n = 10) each time that oxygen gas was supplied. Interestingly, we found that the mesh patterns were not strictly specific to individual cells but varied (e.g., star shaped at first, fern shaped second, and polygonal third) in the same cells, even though the control appearance of cells was recoverable every time. In the other 4 of the 30 cases, the

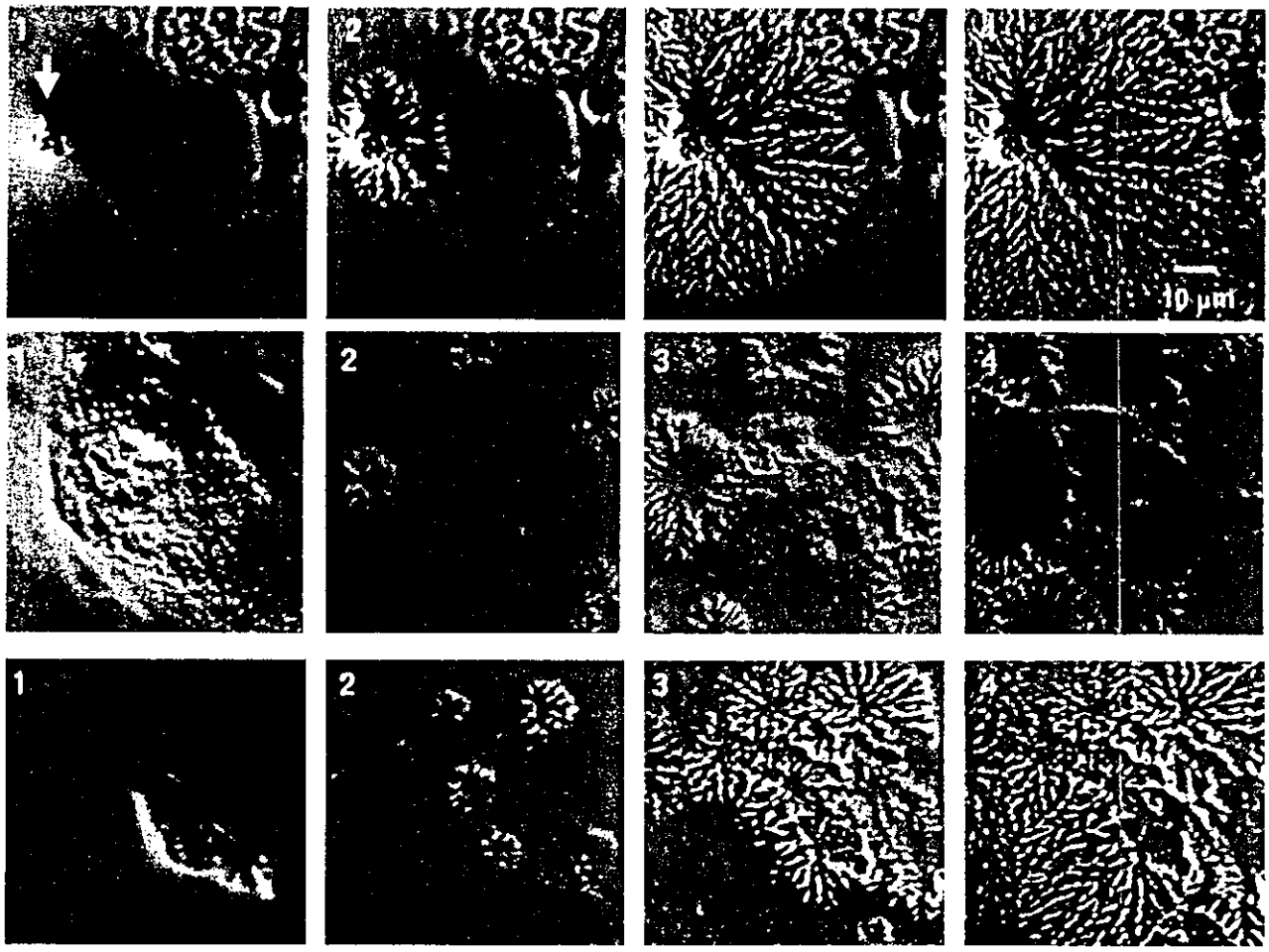

FIG. 3. Formation of a star-shaped mesh network starting from adhesion plaques. The spread speed was 30 μm/s for cell 28 (upper row), 10 μm/s for cell 8 (middle row), and 10 μm/s for cell 11 (bottom row). The arrow in the upper panel indicates a large adhesion plaque, whereas the adhesion plaques in the lower panel (cell 11) were too small to see (if present).

contraction process was similar to that in the abovementioned 26 cases, but there was failure to form a network, and only a clear enhancement of the nuclear envelope was seen (Fig. 3H). Subsequently, small particles appeared in the absence of any detectable fiber network, and the cell underwent a recovery phase as in other cases. Figure 4 (bottom row) illustrates the resolution of a fiber network with a fernlike pattern where the small particles dissolved one by one and disappeared sooner or later, fusing into the cell components.

We confirmed that air blowing did not induce such contraction or the formation of networks. Changes in wall shear rate from 0 to 200 μm/s, and changes in temperature from 10°C to 40°C, also failed to produce contraction/network formation. Electrical stimulation at 0.5 to 3.0 V DC/AC (50 Hz), with a square pulse/triangular pulse at frequencies of 1 to 100 Hz, also failed to produce the previously described morphologic changes, but rather led to an amorphous, disorganized cell structure involving deformation, rounding, and lifting up of the cell body from the floor to which the cell had adhered. These changes were very different from the above-described, clearly defined and organized sequential events.

DISCUSSION

Doukas et al. (1994) observed that endothelial cells cultured on polymerized silicone deformed the underlying substrate, producing microscopically visible wrinkles. They interpreted this finding as being due to cellular contraction, and concluded that endothelial cells normally maintain an active contractile tone. We observed the endothelial tone more directly as wrinkles on the surface of the plasmic membrane: oxygenation induced tensioning and wrinkling of the HBEC plasmic membrane, causing contraction of the cell body by 14%. If we extrapolate this finding to the capillary (an endothelial tube) *in situ*, the endothelial contraction would correspond to the same magnitude of reduction in caliber ($2\Delta R$) based on the simple relation $\Delta D = 2\pi\Delta R$, where ΔD is the change in endothelial cell diameter or the change in the circumferential length of the

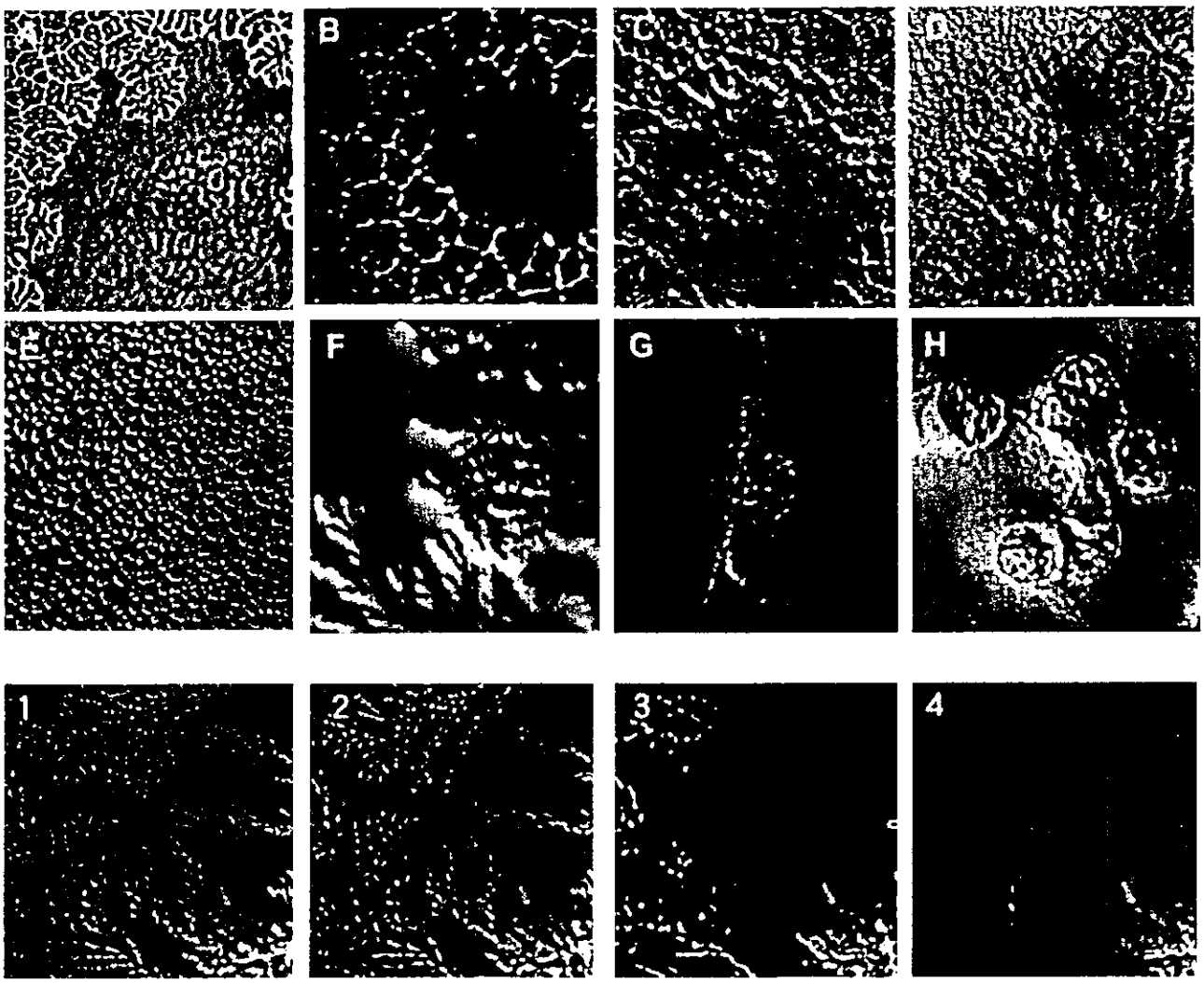

FIG. 4. Top: Various patterns of mesh network structure. (**A**) Star in cell 7. (**B, C**) Polygon in cells 21 and 22. (**D**) Small polygonal in cell 25 near the nucleus. (**E**) Small polygon in the lamella of the same cell 25. (**F**) Fern in cell 5. (**G**) Brush in cell 29. (**H**) Augmented nuclear envelope in cell 3. Bottom: Disassembly and resolution of the fern network structure in cell 6. Particles became detached from the branches of the fern, drifted with Brownian motion, and eventually fused with the intracellular structures.

capillary. In living tissue *in situ,* such active capillary contraction would cause a sharp rise in local capillary flow resistance owing to the inverse Fåhraeus-Lindqvist effect. This may explain the marked reduction in blood flow in response to oxygen inhalation in experimental animals, in the absence of any appreciable pial arterial diametric constriction.

Concerning the stimulus applied to the HBEC, we do not consider oxygen to be the only stimulus that might elicit such rapid changes in endothelial morphology or capillary tone, although changes in various physical factors in our experimental design (e.g., temperature, shear rate, electrical field potential, and surface vibration) had no apparent effect. In the literature, there are reports of numerous triggering stimuli, including not only chemical substances but also such longstanding physical stresses as fluid shear stress (Azuma et al., 2001; Barbee et al., 1994; Frame and Sarelius, 2000; Malek and Izumo, 1996; Schnittler et al., 1993;), stretching *per se* (Sugimoto et al., 1995; Wang et al., 2000; Zhao et al., 1995), and contact with leukocytes (Tomita et al., 1996*b*; Yuan et al., 2002) or lymphocytes (Etienne-Manneville et al., 2000). Chien and Shyy (2001) found that integrins on the abluminal side and receptor tyrosine kinases on the luminal side of endothelial cells serve as mechanosensors. Endothelial and therefore capillary tone changes in response to various stimuli must be of physiologic importance for capillary vasomotion.

The mechanism of the HBEC contraction could be related to spontaneous fiber network formation. However, peculiarly, the fibers became apparent only when contraction was almost completed, after beginning at putative adhesion plaques (integrins) and spreading to the whole cell. The fibers are presumably a cytoskeleton,

TABLE 1. *Summary of HBEC changes in response to oxygenation*

No.	Appearance	Duration	Recovery	Fiber thickness	Particle diameter	Speed	Contraction (%)	Mesh
1	4	4	7	0.5	1	NM	10	Brush
2	1	5	2	NM	0.7	NM	14	Aug. nucl. env.
3	1	10	2	1	1	NM	21	Brush
4	2	10	2	1	1	NM	14	Aug. nucl. env.
5	10	25	3	0.75	1	5	9	Fern
6	2	15	20	0.75	0.5	NM	7	Fern
7	3	1	20	0.5	0.5	10	4	Star
8	5	3	15	1	0.5	10	20	Star
9	10	12	20	0.75	0.5	10	12	Polygonal
10	10	30	50	0.75	0.5	30	12	Fern
11	10	6	15	0.75	0.5	10	14	Star
12	13	10	30	0.75	0.75	10	16	Fern
13	2	7.5	10	0.5	0.5	15	20	Polygonal
14	2.5	7.5	12.5	0.5	0.5	10	23	Fern
15	10	7	30	0.75	0.75	15	19	Fern
16	10	5	20	0.75	0.75	15	28	Star
17	1.5	NM	5	NM	NM	NM	4	Aug. nucl. env.
18	2	NM	3	NM	NM	NM	29	Aug. nucl. env.
19	2.5	8	4	0.5	NM	NM	10	Brush
20	5	12	17	1	1	12	4	Fern
21	15	30	10	0.75	0.5	10	12	Polygonal
22	10	11.5	10	0.75	0.5	20	9	Polygonal
23	5	10	8	0.75	0.5	15	9	Star
24	12	10	20	0.75	0.75	15	33	Star
25	5	10	5	0.75	0.5	NM	13	Polygonal
26	15	26	10	0.5	0.5	30	10	Polygonal
27	3	20	5	0.5	0.5	30	13	Star
28	4	13	16	0.5	0.5	30	10	Star
29	15	10	3	0.75	0.5	30	10	Brush
30	5	17	2	0.75	0.5	10	10	Star
Mean	6.5	12.0	12.6	0.7	0.6	16.3	14	—
SD	4.6	7.8	10.8	0.2	0.2	8.4	7	—

Values expressed as s and μm, except for that of speed which is in μm/s.
Aug. nucl. env., augmented nuclear envelop; NM, not measured; HBEC, human brain microvascular endothelial cell.

which might be stress fibers comprising thick bundles of microfilaments lying along the ventral surface of the cell with their ends attached to adhesion plaques. The stress fibers are thought to contain all the elements required for active contraction: myosin, α-actin, and tropomyosin. Caldesmon, a protein regulating the motile interactions of actin and myosin, is concentrated along the margins of such stress fibers (Lodish et al., 1995). Stress fibers are thus classified as contractile, like those in the sarcomere, because they contract on addition of ATP when isolated from the cell (Katoh et al., 1998). The network that we observed is consistent in terms of fiber thickness (<0.6 μm) and manner of formation with the stress fibers reported previously, except for its mesh network appearance. Stress fibers have previously been reported to be straight (Ishida et al., 1999), whereas ours consisted of variable mesh structures. The fibers reported here could consist of actin and vimentin, but this will need to be confirmed by means of cytochemical and immunocytochemical analysis.

Acknowledgments: The authors thank Dr. Maria Spatz (Stroke Branch, NINDS, NIH, U.S.A.) for her critical reading of the manuscript and helpful suggestions.

REFERENCES

Azuma N, Akasaka N, Kito H, Ikeda M, Gahtan V, Sasajima T, Sumpio BE (2001) Role of p38 MAP kinase in endothelial cell alignment induced by fluid shear stress. *Am J Physiol* 280:H189–H197

Barbee KA, Davies PF, Lal R (1994) Shear stress-induced reorganization of the surface topography of living endothelial cells imaged by atomic force microscopy. *Circ Res* 74:163–171

Chien S, Shyy JY (2001) Mechanisms of mechanochemical transduction in vascular cells. In: *Ischemic blood flow in the brain, Keio University Symposium for Life Sciences and Medicine, Vol 6* (Fukuuchi Y, Tomita M, Koto, eds), Tokyo: Springer, pp 13–19

Craigen ML, Jennett S (1981) Pial arterial response to systemic hypoxia in anaesthetised cats. *J Cereb Blood Flow Metab* 1:285–296

Doukas J, Cutler AH, Boswell CA, Joris I, Maino G (1994) Reversible endothelial cell relaxation induced by oxygen and glucose deprivation: a model of ischemia *in vitro*. *Am J Pathol* 145:211–219

Etienne-Manneville S, Manneville JB, Adamson P, Wilbourn B, Greenwood J, Couraud PO (2000) ICAM-1-coupled cytoskeletal rearrangements and transendothelial lymphocyte migration involve intracellular calcium signaling in brain endothelial cell lines. *J Immunol* 165:3375–3383

Frame MD, Sarelius IH (2000) Flow-induced cytoskeletal changes in endothelial cells growing on curved surfaces. *Microcirculation* 7:419–427

Hudetz AG (1997) Regulation of oxygen supply in the cerebral circulation. *Adv Exp Med Biol* 428:513–520

Inoue K, Tomita M, Tanahashi N, Takeda H, Yokoyama M, Fukuuchi Y (1999) Thickness of cultured human umbilical cord vein endothelial cell as measured by VEC-DIC microscopy [abstract]. *Microcirc Annu* 15:59–60

Ishida T, Ishida M, Suero J, Takahashi M, Berk BC (1999) Agonist-stimulated cytoskeletal reorganization and signal transduction at focal adhesions in vascular smooth muscle cells require c-Src. *J Clin Invest* 103:789–797

Katoh K, Kano Y, Masuda M, Onishi H, Fujiwara K (1998) Isolation and contraction of the stress fiber. *Mol Biol Cell* 9:1919–1938

Kety SS, Schmidt CF (1948) The effect of altered arterial tensions of carbon dioxide and oxygen on cerebral blood flow and cerebral oxygen consumption of normal young men. *J Clin Invest* 27:484–492

Krogh A (1918) The rate of diffusion of gases, with some remarks on the coefficient of invasion. *J Physiol* 52:391–408

Lodish H, Baltimore D, Berk A, Zipursky SL, Matsudaira P, Darnell J (1995) Microfilaments, actin and myosin in nonmuscle cells. In: *Molecular cell biology,* New York: *Sci Am* Books, Inc., pp 1032–1035

Malek AM, Izumo S (1996) Mechanism of endothelial cell shape change and cytoskeletal remodeling in response to fluid shear stress. *Cell Sci* 109:713–726

Meyer JS, Gotoh F (1961) Interaction of cerebral hemodynamics and metabolism. *Neurology* 11:46–65

Meyer JS, Gotoh F, Takagi Y (1967) Inhalation of oxygen and carbon dioxide gas: effect on composition of cerebral venous blood. *Arch Int Med* 119:4–15

Opitz E, Schneider M (1950) Über die sauerstoffversorgung des gehirns und den mechanisms von mangelwirkungen. *Ergbn Physiol* 46:126–260

Purves MJ (1972) *The physiology of the cerebral circulation*, Cambridge: Cambridge University Press, pp 232–252

Schnittler HJ, Franke RP, Akbay U, Mrowietz C, Drenckhahn D (1993) Improved *in vitro* rheological system for studying the effect of fluid shear stress on cultured cells. *Am J Physiol* 265:C289–C298

Sjoberg F, Gustafsson U, Eintrei C (1999) Specific blood flow reducing effects of hyperoxaemia on high flow capillaries in the pig brain. *Acta Physiol Scand* 165:33–38

Sugimoto K, Yoshida K, Fujii S, Takemasa T, Sago H, Yamashita K (1995) Heterogeneous responsiveness of the *in situ* rat vascular endothelial cells to mechanical stretching *in vitro. Eur J Cell Biol* 68:70–77

Tomita M, Fukuuchi Y, Tanahashi N, Kobari M, Takeda H, Yokoyama M, Ito D, Terakawa S (1995) Contraction/dilatation of cultured vascular endothelial cells induced by hyperoxia/hypoxia [abstract]. *J Cereb Blood Flow Metab* 15(Suppl 1):S271

Tomita M, Fukuuchi Y, Tanahashi N, Kobari M, Takeda H, Yokoyama M, Ito D, Terakawa S (1996*a*) Swift transformation and locomotion of PMNL and microglia as observed by VEC-DIC microscopy. *Keio J Med* 45:213–224

Tomita M, Fukuuchi Y, Tanahashi N, Takeda H, Yokoyama M, Haapaniemi H. (1996*b*) Disruption of membranous monolayers of cultured pig and rat brain endothelial cells induced by activated human polymorphonuclear leukocytes. In: *Biology and physiology of the blood-brain barrier* (Courud PO, ed), New York: Plenum Press, pp 253–261

Wang JH, Goldschmidt-Clermont P, Yin FC (2000) Contractility affects stress fiber remodeling and reorientation of endothelial cells subjected to cyclic mechanical stretching. *Ann Biomed Eng* 28:1165–1171

Yuan SY, Wu MH, Ustinova EE, Guo M, Tinsley JH, De Lanerolle P, Xu W (2002) Myosin light chain phosphorylation in neutrophil-stimulated coronary microvascular leakage. *Circ Res* 90:1143–1144

Zhao S, Suciu A, Ziegler T, Moore JE Jr, Burki E, Meister JJ, Brunner HR (1995) Synergistic effects of fluid shear stress and cyclic circumferential stretch on vascular endothelial cell morphology and cytoskeleton. *Arterioscler Thromb Vasc Biol* 15:1781–1786

特集／脳卒中 — 診断と治療のめざましい進歩

脳卒中治療の現況とその進歩

急性期治療における脳保護薬の適応と効果

棚橋紀夫

はじめに

脳梗塞急性期の治療は，血栓溶解療法，抗凝固療法・抗血小板療法などの抗血栓療法と神経細胞を保護する脳保護療法に大別される[1]。後者は，神経細胞のみでなく，アストロサイト，オリゴデンドロサイト，血管内皮細胞の保護も重視されるようになり神経細胞保護というよりは脳保護と表現される。これらの治療法のうち超急性期における血栓溶解療法が最も効果が期待できる治療法であるが，出血性合併症を伴うことがあり症例の選択が重要な課題である。抗凝固薬，抗血小板薬は，アルガトロバン，オザグレルのように本邦で開発され広く使用されるようになった薬剤もあり，微小循環の改善を介し脳梗塞の治療成績改善に寄与している。一方，脳保護薬は，後述する虚血性神経細胞障害の機序が，動物実験により次第に解明され臨床試験が行われたが，効果が認めなかったもの，副作用がみられたものなどが多かった。その中で，フリーラジカルスカベンジャーの一種であるエダラボンが，唯一本邦で脳梗塞保護薬として認可され，広く使用されるに至っている。

Ⅰ．虚血性神経細胞障害の機序

虚血性神経細胞障害は，虚血の程度と持続時間によって決まる。虚血中心部で虚血の程度が強い場合は比較的単時間にネクローシスをきたし梗塞になる。一方，虚血の程度の軽い場所（虚血周辺部あるいはペナンブラ）では，血流回復により梗塞にならない場合もあれば，時間とともにアポトーシスにより梗塞に移行する場合がある。したがって，虚血性神経細胞障害の機序は，障害の程度・部位によりそのメカニズムが異なる。さらに血流が再開通した場合は再潅流障害を来す場合がある。

図1に虚血発生後の時間経過と各種虚血性脳損傷メカニズムの発生の関係を虚血部位と関連して示す[2]。虚血発生直後の虚血中心部では，虚血性脱分極と，灰白質に存在する神経細胞体と樹状突起ではグルタミン酸やCa^{2+}，白質ではNa^{+}が重要な役割を果たしている。虚血周辺部では，虚血発生にやや遅れてフリーラジカル産生に伴う酸化的障害（oxidative injury），二次的血栓形成などによる微小循環障害，多核白血球とマクロファージの浸潤やcyclooxygenase2活性化などの炎症性反応，アポトーシスによる細胞死機転が働く。また，虚血病変拡大を抑制するかのように種々の内在性保護機転に基づく修復反応が賦活化される。図2には虚血性神経細胞障害の発生機序を主に分子機構の面から示す[3]。脳虚血が発生すると脳組織はエネルギー不全となり，ATPが枯渇，Na/K

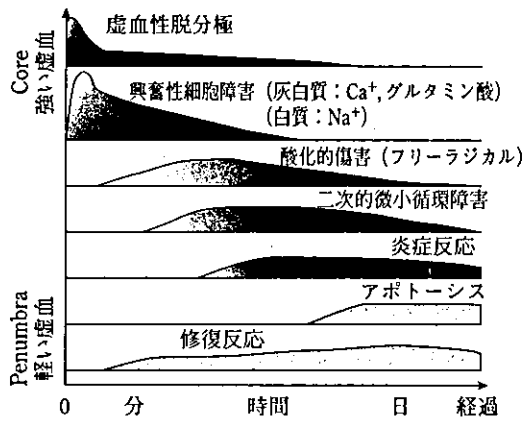

図上段のメカニズムほど虚血巣中心部で生じ，下段のものほど周辺部で生ずる。

図　1　虚血開始後の時間経過と各種虚血性脳損傷メカニズム発生の関係（文献2より引用）

慶應義塾大学医学部神経内科　講師

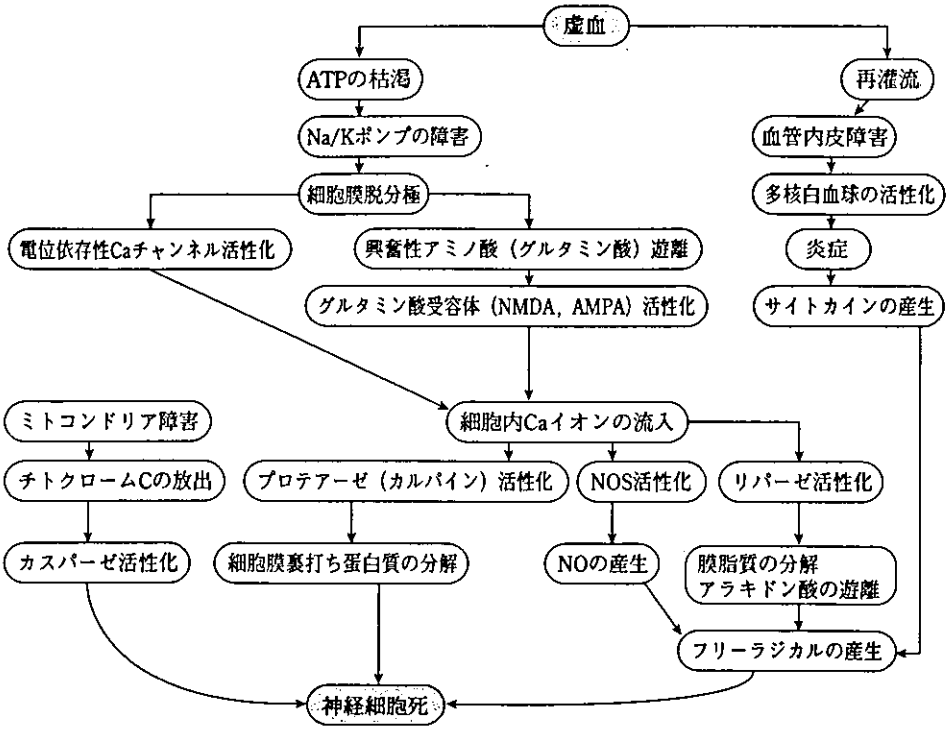

図　2　虚血性神経細胞障害の発生機序（文献3より引用）

ATPaseが作動しなくなり細胞内へのNa流入，細胞膜脱分極，興奮性アミノ酸の放出，細胞内へのカルシウムイオンの流入が相次いで連鎖して生じていく。細胞内カルシウムの上昇は，カルパインをはじめとしたプロテアーゼの活性化，リパーゼの活性化により細胞骨格蛋白質，脂質膜の崩壊を引き起こす。Ca依存性の一酸化窒素合成酵素の活性化によりNOが産生される。重度の虚血状態が遷延すればこのまま細胞崩壊へ至ると考えられるが，虚血周辺部で残存血流のある領域や血流再開通により再酸素化が生じると，損傷を受けたミトコンドリアからの電子遊離，膜脂質分解により活性化されたアラキドン酸代謝カスケードに酸素が反応することによりフリーラジカルが産生され，その量が多ければ膜脂質過酸化，蛋白質カルボニル化，DNA損傷を引き起こし細胞を障害する。さらに細胞内Caイオン負荷，フリーラジカルの産生のため，ミトコンドリアからのチトクロームCの遊離が生じ，カスパーゼ9，3の活性化が引き起こされATPの存在下ではアポトーシスの分子機構も発動するようになる。

Ⅱ．脳保護薬の開発状況

表1に臨床試験で評価されたまたは評価中の主な脳保護薬の一覧を示す[4]。

グルタミン酸受容体拮抗薬，GABA作動薬，Caチャンネル拮抗薬，Naチャンネル拮抗薬，フリーラジカル消去薬，細胞膜安定化薬，白血球粘着阻害薬，成長因子などが検討されてきたが，フリーラジカル消去薬を除いて殆ど有効性が実証されなかった。その理由として，まず実験動物，特にげっし類とヒト脳組織との構造の違いがある。ラット，マウスでは灰白質にくらべ白質が小さい。灰白質の主要な構成要素である神経細胞には，電位依存性Ca^{2+}チャンネルが存在し，多数のグルタミン酸作動性神経線維がシナプスを形成し，シナプス後膜側にはNMDA受容体などのグルタミン酸受容体が集積している。一方，白質の主要な構成要素である神経線維の軸索はミエリンで覆われ，Ranvier絞輪部では電位依存性Na^+チャンネルが高密度で存在し，Na^+-K^+-ATPaseも多く存在する[5]。しかし，同部にはNMDA受容体などのグルタミン酸受容体や電位依存性Ca^{2+}チャンネルは存在しない。またオリゴデンドロサイトにはグルタミン酸受容体としてNMDA受容体は存在せず，AMPA/kainate受容体のみ存在している[6]。そのためNMDA受容体拮抗薬のような灰白質，とくに神経細胞に対してのみ保護効果が期待される薬剤は，ラットやマウスでは有効でも，白質に脳梗塞が多いヒトでは有効性は少なくなる可能性

表　1　最近臨床試験で評価されたまたは評価中の脳保護薬

薬物の分類	薬剤名	作用機序	臨床試験
グルタミン酸拮抗薬			
NMDA 受容体拮抗薬	aptiganel	NMDA チャンネル阻害	無　効
	dextrorphan		無　効
	CGS 19755	競合阻害	有　害
	GV 150526	グリシン結合部位阻害	無　効
	SL 82-0715	ポリアミン結合部位阻害	無　効
AMPA 受容体拮抗薬	YM872		進行中
GABA 作動薬	clomethiazole	神経興奮抑制	無　効
Na チャンネル拮抗薬	fosphenytoin	興奮，グルタミン酸抑制	無　効
Ca チャンネル拮抗薬	nimodipine	カルシウム流入抑制	無　効
K チャンネル刺激薬	BMS-204352	カルシウム流入抑制	無　効
ラジカル消去薬	tirilazad mesylate	フリーラジカル障害の抑制	無　効
	ebselen		無　効
	edaravone		有　効
	nicaravone		有　効
細胞膜安定化薬	citicholine	神経細胞膜修復	無　効
神経栄養因子	FGF		無　効
白血球粘着抑制薬	抗 ICAM-1 抗体	白血球粘着阻害	無　効
その他	lubeluzole		無　効
	ONO-2506	アストロサイト機能改善	進行中

がある[7]。その他，動物実験では，虚血時間，虚血の程度，再潅流の有無，薬物投与時間などを十分コントロールできるが，ヒトでは脳梗塞の病型，虚血程度，持続時間，危険因子の有無などの諸条件に大きな差があることが多い。また，ヒトにおける臨床試験の endopoint は，発症90日目の機能予後（modified Rankin Scale）が一般的であるが，梗塞巣の縮小が臨床症状の改善度の違いとしてあらわれるかどうか，評価方法などの根本的問題もある。さらに，発症後6時間位までに本来梗塞となる部位の殆どが梗塞になっており，ペナンブラの領域，存在時間が予想以上に短く，脳保護療法で恩恵を受けにくい可能性も指摘されている[8]。また副作用として，グルタミン酸受容体拮抗薬での幻覚・興奮状態などの中枢神経症状の出現，イオンチャンネル阻害薬での徐脈・不整脈などの心血管系の症状発現が問題となった。

Ⅲ．フリーラジカルスカベンジャー・抗酸化薬

1．脳虚血の病態におけるフリーラジカル・活性酸素種

核の周囲を回る軌道に一個しか電子がない状態（不対電子）をもつ物質をフリーラジカルと呼ぶ。フリーラジカルは不対電子が対になろうとして他の物質から電子を奪い取ろうとするために反応性が高い。すなわち相手を酸化する力が強い物質がフリーラジカルということになる。生体に存在するフリーラジカルは，活性酸素の仲間であるスーパーオキシドとヒドロキシラジカル，一酸化窒素（NO），過酸化脂質などがある（表2）。それらが，細胞やミトコンドリアの膜，DNA，蛋白，レセプターの主要な構成物である糖鎖，酵素をターゲットとしてこれらを酸化すれば個々の機能が失われ，結果的に細胞障害がおこることになる。特に脳は細胞膜脂質に不飽和脂肪酸を多く含むため，虚血によるフリーラジカルの攻撃を受けやすい。生理的状態でも，1～3％の酸素が活性酸素（フリーラジカルであるスーパーオキシドと活性酸素種のひとつである過酸化脂質）に変換されるとい

表　2　活性酸素種 reactive oxygen species (ROS)

1．フリーラジカル
　分　子：superoxide（$\cdot O_2^-$）
　　nitric oxide（$\cdot NO$）
　　nitric dioxide（$\cdot NO_2$）
　原子団：hydroxy radical（$\cdot OH$）
　　alkoxyl radical（$\cdot LO$）
　　peroxyl radical（$\cdot LOO$）
　　L：lipid
2．その他
　hydrogen peroxide（H_2O_2）過酸化水素
　peroxynitrite（$ONOO^-$）
　singlet oxygen（$^1O_2$）
　hydroperoxide（LOOH）過酸化脂質

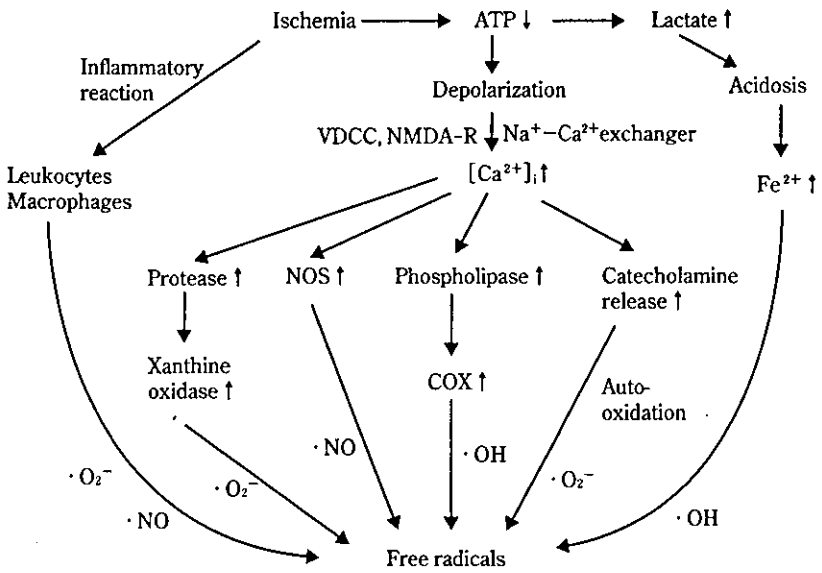

(NOS：一酸化窒素合成酵素，COX：シクロオキシゲナーゼ)

図　3　　虚血時のフリーラジカル発生機序（文献2より引用）

われている。そのためフリーラジカルに対する防御システムが生体には備わっており，フリーラジカルを変化させて反応性のないものにする酵素と，自分が標的となり酸化されてフリーラジカルの酸化作用を消去する抗酸化物質に分けられる。酵素としてはスーパーオキシドジスムターゼ（SOD），グルタチオンパーオキシダーゼ，カタラーゼがあるが脳では前二者が主たるものである。抗酸化物質としては，水溶性でビタミンC，還元型グルタチオン，ビリルビン，尿酸が挙げられ，脂溶性ではビタミンE，βカロチンが挙げられる。生理的に発生するスーパーオキシドと過酸化水素は防御系で十分消去されるが，虚血－再潅流により防御システムが破綻したり，処理しきれないほどの量が生成されると反応性に富むヒドロキシラジカルが生成される。しかも，このヒドロキシラジカルを消去するシステムを生体をもっていないので細胞障害をきたすことになる[9]。

図3に虚血時のフリーラジカルの発生機序を示す。活性酸素種やフリーラジカルは，虚血時には脳内で各種実質内細胞のみならず血管内皮細胞や白血球でも産生される。脳虚血時に脳内で産生される代表的フリーラジカルはスーパーオキシドである。生体内ではスーパーオキシドジスムターゼ（SOD）やグルタチオンパーオキシダーゼの働きで無毒化されるが，Fe^{2+}のような二価の金属イオンがあったりその他の遷移金属が存在すると，fenton反応やHaber-Weiss反応によって一層強力なフリーラジカルであるヒドロキシラジカルに変化する。また，スーパーオキシドはSODよりもNOに対してより親和性が高く，両者は反応してパーオキシナイトライトを産生するが強い細胞毒性を示す。

2.　脳梗塞急性期治療薬としてのフリーラジカルスカベンジャー

エダラボン

エダラボンはヒドロキシラジカル補捉作用，脂質過酸化やリポキシゲナーゼ抑制効果を有する。さらにエダラボンの特徴として小分子であるため脳に到達できること，生体膜と脂質側の界面近くに存在するためにビタミンEやビタミンCと優れた相乗抗酸化効果を示すことがあげられる[10]。

発症72時間以内，意識障害が3-3-9度方式で0-30，の脳梗塞急性期患者を対象とした二重盲検試験が行われた[11]。総投与症例は252例で2群に分けられ，エダラボン群125例とプラセボ群127例であった。エダラボン群では，エダラボン30mgの1日2回点滴静注を14日間行った。基礎治療薬としてグリセロールを1日400～600ml併用し，エダラボン群の薬効に影響を及ぼす薬剤，すなわちオザグレル，ヘパリンなどの使用は避けた。このうち発症24時間以内に治療を開始した症例は，エダラボン群42例，プラセボ群39例であった。その結果，発症より3ヵ月後ないしそれ以前に退院した症例では退院時の機能評価予後（modified Rankin scale）では，表3のようにgrade 0の全

表 3　発症24時間以内に治療された患者の3ヵ月以内の退院時の modified Rankin Scale

グレード	エダラボン群 (n＝42)	プラセボ群 (n＝39)
0	14	1
1	10	6
2	8	13
3	5	3
4	2	4
5	2	4
死亡	1	4
	p＝0.0001*	

*Wilcoxon's rank sum test

く症状なしの症例がエダラボン群14例（34.1%）でプラセボ群の1例（2.9%）に比し有意に多かった。さらに，最終全般改善度の梗塞部位別解析で，穿通枝のみの症例では改善以上を示した症例がエダラボン群では12例中11例，プラセボ群では12例中4例のみでエダラボンで有意に多かった。一方，皮質枝を含む症例では改善以上を示した症例が11例中7例，プラセボ群では13例中2例であり両群間に統計的に有意差はなかった。この結果はエダラボン群が特に白質の梗塞病変に有効であることを示唆している。この結果をもとに，世界で初めて脳保護薬として発症24時間以内の脳梗塞患者に2001年より使用認可された。白質が理論的にフリーラジカル障害を受けやすいとされている。それは，白質の重要な構成要素であるミエリン成分の80%は脂肪であり，脂質過酸化によるフリーラジカル障害を受けやすいこと，オリゴデンドロサイト自体も内因性抗酸化物質であるグルタチオン濃度が低く，フェリチンなどの鉄含有量が多いことなどによる。

エダラボンを使用する場合注意すべきことは，腎毒性の問題である。腎障害のある患者，特に高齢者では腎機能のチェックを十分に行う必要がある。

エダラボン認可以後の臨床的検討では，エダラボン使用により血栓溶解療法施行時の血腫形成を減少させるとする報告が注目されている[12]。

3.　その他のフリーラジカルスカベンジャー

グルタチオンペルオキシダーゼ様作用とリポキシゲナーゼ抑制作用があり強力な抗酸化薬であるエブセレンは，臨床的にも有効性が証明され[13]，基礎実験でも興味深い結果[14]が報告された。しかし，再度の第Ⅲ相臨床試験で有効性が証明されなかった。ヒドロキシラジカル補捉作用を有するニカラベンも脳梗塞に対する臨床試験が終了しているがいまだ認可には至っていない。この他にも，新しいフリーラジカルスカベンジャーが開発されつつある。

Ⅳ. 脳梗塞ガイドラインにおける脳保護薬の位置付け

2003年度に米国脳卒中協会からでた虚血性脳卒中の初期管理ガイドラインの改訂版[15]によると，現時点では，虚血性脳卒中急性期に推奨できる脳保護薬はない（グレードA）とされている。一方，本邦の脳卒中合同ガイドライン委員会で作成された“脳卒中治療ガイドライン2003”[16]では脳梗塞（血栓症，塞栓症）急性期の治療法として脳保護作用が期待される薬剤（エダラボン）を投与することが勧められる（グレードB）とされている。

Ⅴ. 今　後　の　展　望

脳保護薬の多くが，臨床試験の段階で有効性を否定されたり，有害事象の出現のため開発を断念されたことは多くの臨床医を落胆させた。さらに製薬業界の脳保護薬の開発に対する意欲を低下させた。しかし，本邦でフリーラジカルスカベンジャーであるエダラボンが認可されたことは脳保護薬の将来に一条の光を照らした。脳梗塞急性期の治療は，血栓溶解療法，脳浮腫療法などと脳保護療法の併用の時代になった。虚血性神経細胞障害の分子機構がさらに詳細に明らかになるにつれ，脳保護療法の更なる発展が期待される。

参　考　文　献

1) Tanahashi, N., Fukuuchi, Y.: Treatment of acute ischemic stroke: Recent progress. Internal Medicne, 41: 337-344, 2002.
2) 田中耕太郎：脳梗塞．急性期の病態．虚血性脳組織損傷のメカニズム．神経内科，58(Suppl 3)：116-131，2003.
3) 北川一夫，松本昌泰：脳梗塞．急性期の病態．脳保護療法．神経内科，58(Suppl 3)：283-293，2003.
4) Lee, J.-M., Grabb, M. C., Zipfel, G. J., Choi, D. W.: Brain tissue responses to ischemia. J Clin Invest, 106(6): 723-731, 2000.
5) Ellisman, M., Deerinck, T., Bennett, V.: Structure and formation of the node of Ranvier. In Glial cell development (edited by Jessen, K. R. & Richrdson, W. D.), Oxford University Press, Oxford, pp131-160, 2001.
6) Baumann, N., Pham-Dinh, D.: Biology of oligodendrocyte and myelin in the mammalian central nervous system. Physiol Rev, 81: 871-927, 2001.
7) Dewar, D., Yam, P., McCulloch, J.: Drug develop-

ment for stroke: importance of protecting cerebral white matter. Eur J Pharmacol, 375: 41-50, 1999.
8) Heiss, W.-D., Kracht, L. W., Thiel, A., Grond, M., Pawlik, G.: Penumbral probability thresholds of cortical flumazenil binding and blood flow predicting tissue outcome in patients with cerebral ischaemia. Brain, 124: 20-29, 2001.
9) 山本清二: 脳虚血に対する抗酸化薬. Brain Rescue, 1: 11-13, 2002.
10) Yamamoto, Y. et al.: Antioxidant activity of 3-methyl-1-phenyl-2-pyrazolin-5-one. Redox Report, 2(5): 333-338, 1996.
11) Edaravone Acute Infarction Study Group: Effect of a novel free radical scavenger, edaravone (MCI-186), on acute brain infarction. Randomized, placebo-controlled, double-blind study at multicenters. Cerebrovasc Dis, 15(3): 222-229, 2003.
12) 小林祥泰: 超急性期脳梗塞における血栓溶解療法と脳保護薬（エダラボン）の併用効果. "脳卒中データバンク" 小林祥泰編集, 中山書店, pp66-67, 2003年3月発行.
13) Yamaguchi, T., Sano, K., Takakura, K., Saito, I., Shinohara, Y., Asano, T., Yasuhara, H.: Ebselen in acute ischemic stroke: a placebo-controlled, double-blind clinical trial. Stroke, 29: 12-17, 1998.
14) Imai, H., Masayasu, H., Dewar, D., Graham, D. I., Macrae, I. M.: Ebselen protects both gray and white matter in a rodent model of focal cerebral ischemia. Stroke, 32: 2149-2154, 2001.
15) Adams, H. P. et al.: Guidelines for the early management of patients with ischemic stroke: A scientific statement from the Stroke Council of the American Stroke Association. Stroke, 34: 1056-1083, 2003.
16) 脳卒中合同ガイドライン委員会: 脳卒中治療ガイドライン2003, 興和印刷株式会社, 2003年5月15日発行.

アテローム血栓性脳梗塞

棚橋 紀夫

頻 度

脳内や頸部の大血管の粥状硬化に起因するアテローム血栓性脳梗塞の発症機序には，血栓性 thrombotic，塞栓性 embolic (artery-to-artery embolism)，血行力学的 hemodynamic (watershed infarction) の3つの場合がある．artery-to-artery embolism (動脈原性脳塞栓症) は，動脈硬化性粥腫に付着した血栓または粥腫断片が剝がれ，遠位脳動脈での塞栓を生じるものである．NINDS による CVD-III の分類[1]の臨床分類では，アテローム血栓性脳梗塞に分類される．近年，アテローム血栓性脳梗塞は，その頻度が増加しているといわれている．図1に脳梗塞急性期医療の実態に関する研究 (平成12年度研究報告)[2]の頻度を示す．図2に Japan Standard Stroke Registry Study (2002) による脳卒中病型別頻度を示す[3]．この統計により動脈原性脳塞栓症の頻度が明らかとなった．図3に，久山町調査[4]での脳梗塞の病型別の時代的変化を示す．男性で時代とともにアテローム血栓性脳梗塞が増加しており，日本人の脳梗塞が欧米化の方向に向かっていることを示している．

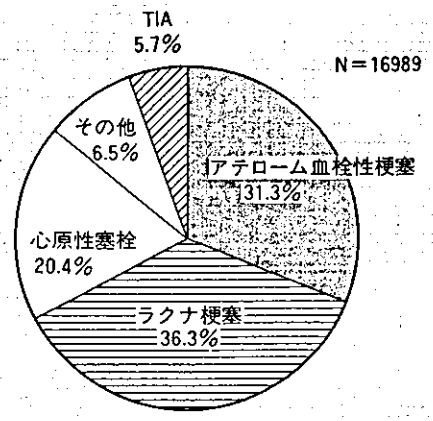

図1 脳梗塞の病型別頻度 (脳梗塞急性期医療の実態に関する研究．平成12年度研究報告[2])

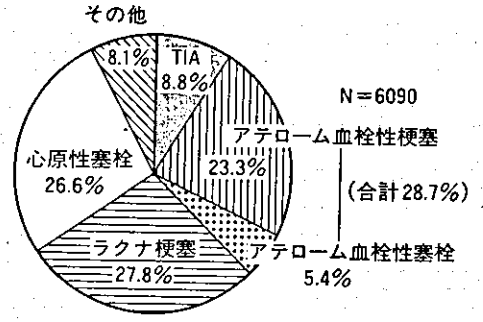

図2 虚血性脳卒中の病型別頻度 (JSSRS 2001，小林[3])

危険因子

表1に，Japan Standard Stroke Registry Study (2002) による脳梗塞臨床病型別にみた脳梗塞危険因子の合併頻度

たなはし のりお 慶應義塾大学講師/神経内科

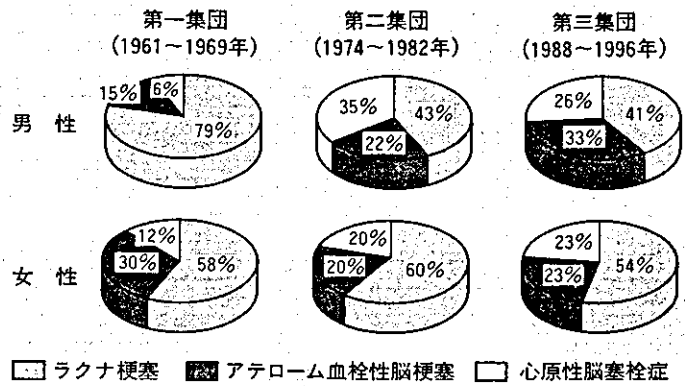

図3 脳梗塞発症例のタイプ別内訳の時代的変化 (久山町3集団，65歳以上，追跡各8年) (清原[4])

0289-0585/03/¥500/論文/JCLS